The Astronomical Journal, 169:272 (8pp), 2025 May https://doi.org/10.3847/1538-3881/adc56a

A Heliocentric-orbiting Objects Processing System (HOPS) for the Wide Field Survey Telescope: Architecture, Processing Workflow, and Preliminary Results

Shao-Han Wang[1,2,10], Bing-Xue Fu[1,2,10], Jun-Qiang Lu[1,2,10], LuLu Fan[1,2,3], Min-Xuan Cai[1,2], Ze-Lin Xu[1,2], Xu Kong[1,2,3], Haibin Zhao[2,4], Bin Li[4], Ya-Ting Liu[5], Qing-feng Zhu[1,2,3], Xu Zhou[6], Zhen Wan[1,2], Jingquan Cheng[4], Ji-an Jiang[1,7], Feng Li[8], Ming Liang[9], Hao Liu[8], Wentao Luo[3], Zheng Lou[4], Hairen Wang[4], Jian Wang[3,8], Tinggui Wang[1,2,3], Yongquan Xue[1,2], Hongfei Zhang[8], and Wen Zhao[1,2]

[1] Department of Astronomy, University of Science and Technology of China, Hefei 230026, People's Republic of China; llfan@ustc.edu.cn, xkong@ustc.edu.cn
[2] School of Astronomy and Space Science, University of Science and Technology of China, Hefei 230026, People's Republic of China
[3] Deep Space Exploration Laboratory, Hefei 230088, People's Republic of China
[4] Purple Mountain Observatory, Chinese Academy of Sciences, Nanjing, 210023, People's Republic of China
[5] School of Artificial Intelligence and Data Science, University of Science and Technology of China, Hefei, 230026, People's Republic of China
[6] Key Laboratory of Optical Astronomy, National Astronomical Observatories, Chinese Academy of Sciences, Beijing 100101, People's Republic of China
[7] National Astronomical Observatory of Japan, 2-21-1 Osawa, Mitaka, Tokyo 181-8588, Japan
[8] State Key Laboratory of Particle Detection and Electronics, University of Science and Technology of China, Hefei 230026, People's Republic of China
[9] National Optical Astronomy Observatory (NSF's National Optical-Infrared Astronomy Research Laboratory), 950 N Cherry Ave., Tucson, AZ 85726, USA
Received 2025 January 28; revised 2025 March 20; accepted 2025 March 24; published 2025 April 24

Abstract

Wide-field surveys have markedly enhanced the discovery and study of solar system objects. The 2.5 m Wide Field Survey Telescope (WFST) represents the foremost facility dedicated to optical time-domain surveys in the Northern Hemisphere. To fully exploit WFST's capabilities for solar system object detection, we have developed a heliocentric-orbiting objects processing system (HOPS) tailored for identifying these objects. HOPS integrates HelioLinC3D, an algorithm well suited for the WFST survey cadence, characterized by revisiting the same sky field twice on the majority of nights. In this paper, we outline the architecture and processing flow of HOPS. The application of HOPS to the WFST pilot survey data collected between 2024 March and May demonstrates exceptional performance in terms of both temporal efficiency and completeness. A total of 658,489 observations encompassing 38,520 known asteroids have been documented, and 241 newly discovered asteroids have been assigned provisional designations. In particular, 27% of these new discoveries were achieved using merely two observations per night on three nights. The preliminary results not only illuminate the effectiveness of integrating HelioLinC3D within HOPS, but also emphasize the considerable potential contributions of WFST to the field of solar system science.

Unified Astronomy Thesaurus concepts: Asteroids (72); Small Solar System bodies (1469); Astronomy data analysis (1858); Sky surveys (1464); Heliocentric orbit (706)

1. Introduction

Solar system objects (SSOs) represent remnants from the initial stages of solar system formation. Early evolutionary processes like planetary migration left their imprints in the distributions of the orbital parameters, chemical compositions, and size distributions of the SSOs. The dynamical properties of the different populations have given rise to numerous models of planetary formation and evolution (R. Gomes et al. 2005; A. Morbidelli et al. 2005; K. Tsiganis et al. 2005; K. J. Walsh et al. 2011; S. N. Raymond & A. Izidoro 2017). They include small natural entities within the solar system, ranging in size from ∼1 m to several hundred kilometers, such as near-Earth objects (NEOs), main-belt asteroids, trans-Neptunian objects (TNOs), and various other smaller groups of asteroids and comets (P. Michel et al. 2015; Q. Ye et al. 2019). The study of these objects provides significant insight into the formation and evolution of planets, the potential dangers posed by near-Earth asteroids and comets (P. Brown et al. 2013), and the origins of life and essential life-supporting materials, such as water (Q. Ye 2024).

Wide-field surveys, including the Panoramic Survey Telescope and Rapid Response System (Pan-STARRS; L. Denneau et al. 2013), the Catalina Sky Survey (E. J. Christensen et al. 2016), and the Zwicky Transient Facility (ZTF; F. J. Masci et al. 2018), have facilitated a marked increase in the discovery of SSOs. As of mid 2024, approximately 1.4 million minor planets have been cataloged, including asteroids and 5000 comets (Q. Ye 2024). However, millions of SSOs remain unexplored and await future direct observations (M. E. Schwamb et al. 2018). Furthermore, characterization of these objects in terms of their physical and compositional properties lags significantly, due to the considerable efforts required and the expansive parameter space between identification and physical characterization (M. Mahlke et al. 2019).

Wide Field Survey Telescope (WFST) is a time-domain survey facility located at the summit of Saishiteng Mountain, close to Lenghu Town, in Qinghai Province, dedicated to monitoring dynamic northern skies. Equipped with a 2.5 m diameter primary mirror, an active optics system and a mosaic CCD camera featuring 0.73 gigapixels in the primary focal plane, WFST captures high-quality images over a 6.5 square degree (T. Wang et al. 2023). The telescope benefits from

[10] These authors contributed equally.

excellent observing conditions, including an average seeing of $0\farcs75$ and a background of 22.0 mag arcsec^{-2}, ensuring high-quality data (L. Deng et al. 2021). It achieves a 5σ detection limits of 22.31, 23.42, 22.95, 22.43, 21.50, and 23.61 mag with exposures of 30 s in the u, g, r, i, z, and w bands, respectively (L. Lei et al. 2023). WFST is designed to survey the northern sky with unprecedented sensitivity, aiming to explore the variable universe and catch up the time-domain events, such as supernovae (M. Hu et al. 2023), tidal disruption events (Z. Lin et al. 2022), optical counterparts of gravitational wave events (Z.-Y. Liu et al. 2023), active galactic nuclei (Z.-B. Su et al. 2024) variability, variable stars (J. Lin et al. 2024), and SSOs (J.-Q. Lu et al. 2025). It is anticipated that the WFST will obtain comprehensive observations of known SSOs and identify fainter and smaller bodies, thereby improving our understanding of the solar system (T. Wang et al. 2023; J.-Q. Lu et al. 2025).

To maximize SSO detection in the WFST data, an algorithm must align with the WFST survey cadence, which avoids consecutive single-band observations and instead uses two bands on most nights (T. Wang et al. 2023). This strategy introduces distinct challenges compared to traditional SSO search algorithms like the Pan-STARRS Moving Object Processing System (L. Denneau et al. 2013), which require at least three detections per tracklet. HelioLinC, a multi-night-linking algorithm originally developed for LSST (M. J. Holman et al. 2018), provides an optimal solution for WFST. WFST and LSST, both employing a two-returns-per-night cadence characteristic of wide-field surveys, enable direct algorithmic compatibility, with WFST monitoring the northern hemisphere and LSST focusing on the southern hemisphere. HelioLinC links detections within the same night to form tracklets and connects internight tracklets to create "tracks," typically with a separation of 3–4 nights between adjacent tracklets (LSST Science Collaboration et al. 2009; Ž. Ivezić et al. 2019). The algorithm uses a heliocentric distance and its rate of change to propagate tracklets to a common epoch, forming high-confidence clusters. It covers various asteroid populations from NEOs to TNOs, with minimal computational expense, scaling as $\mathcal{O}$ ($N\log N$) with the number of tracklets N. Notably, initial Isolated Tracklet File (ITF) results demonstrate a purity and accuracy exceeding 99% (M. J. Holman et al. 2018), while its successful implementation with Pan-STARRS1 further corroborates its efficacy (J. A. Kurlander et al. 2025).

This paper presents a heliocentric-orbiting objects processing system (HOPS) tailored for WFST, constructed upon the HelioLinC algorithm, herein referred to as HOPS. The paper is organized as follows. Section 2 details the design and processing of HOPS. In Section 3, HOPS is applied to three months of data from the WFST pilot survey to evaluate its performance and present the preliminary results. Section 4 gives a brief summary.

2. HOPS

Figure 1 illustrates the processing flow of HOPS. After ingesting alert data from the WFST real-time data reduction pipeline, HOPS sequentially performs the following main steps. (1) Preprocess: ingest alert data from the WFST pipeline, match with ephemerides, remove false detections, and automatically inspect known SSOs; (2) single-night processing: identify tracklets, perform visual inspections to confirm candidates; (3) multinight processing: search for pairs and tracklets over a 14 days window, cluster and refine candidates, conduct final visual inspection; (4) submission: perform analysis and quality checks, submit known SSOs from step (1), and confirmed SSO candidates from steps (2) and (3) to the MPC; (5) databases: maintain the databases for HOPS, submissions, orbital, and property data. This section details each processing step.

2.1. Preprocessing

2.1.1. Input Data

Upon obtaining each raw scientific exposure, the WFST real-time data reduction pipeline (M. Cai et al. 2025), which is developed based on the LSST pipeline (M. Jurić et al. 2017), processes the exposure instantaneously. The pipeline systematically performs the following stages. (1) Instrumental signal removal: this involves overscan, bias subtraction, and normalization with the flat images; (2) characterizing image: this step encompasses background estimation and subtraction, source detection, PSF measurement, and cosmic-ray detection and repair; (3) calibrating image: source measurement, aperture correction, astrometric calibration, and photometric calibration are performed; (4) subtracting image: a template image retrieved from coadded images, is subtracted from the calibrated science image, produce a difference image; (5) transient detection and alert distribution: source detection and measurement are performed on the difference image, resulting in a difference source catalog. Then, the source information is associated and presented as alert data, serving as input to HOPS (M. Cai et al. 2025).

2.1.2. Known Asteroids Match

To match known asteroids, HOPS employs `astcheck`[11], using the daily updated MPCORB dataset[12] from the MPC and JPL DASTCOM comet elements.[13] The `astcheck` calculates the ephemerides of known SSOs and cross-matches them with all observations using a 9″ radius threshold. Each source is annotated with its match results: given the corresponding SSO designation with the calculated magnitude $V_{\rm ast}$, or marked as "unknown" if no match is found.

2.1.3. False Detection Removal

We use `braai` (D. A. Duev et al. 2019), a CNN model designed to classify real/bogus sources in ZTF, to identify moving objects and remove false detections in HOPS. Real moving objects should appear in both science and difference images, but not in reference images. Only science images were used in the model due to unreliable difference image processing during the early observation phase. Our dataset includes 4272 true sources and 6269 false sources (see Figure 2), extracted as 50×50 pixel cutouts and manually labeled. These cutouts were divided into training and test sets in a 9:1 ratio. After 100 epochs, the model achieved a loss of 0.0369 and an accuracy of 0.9890. The criteria for genuine moving objects are: science image score $\geqslant$0.55 and reference image score $\leqslant$0.45.

[11] https://www.projectpluto.com/astcheck.htm
[12] http://www.minorplanetcenter.org/iau/MPCORB.html
[13] http://ssd.jpl.nasa.gov/dat/ELEMENTS.COMET

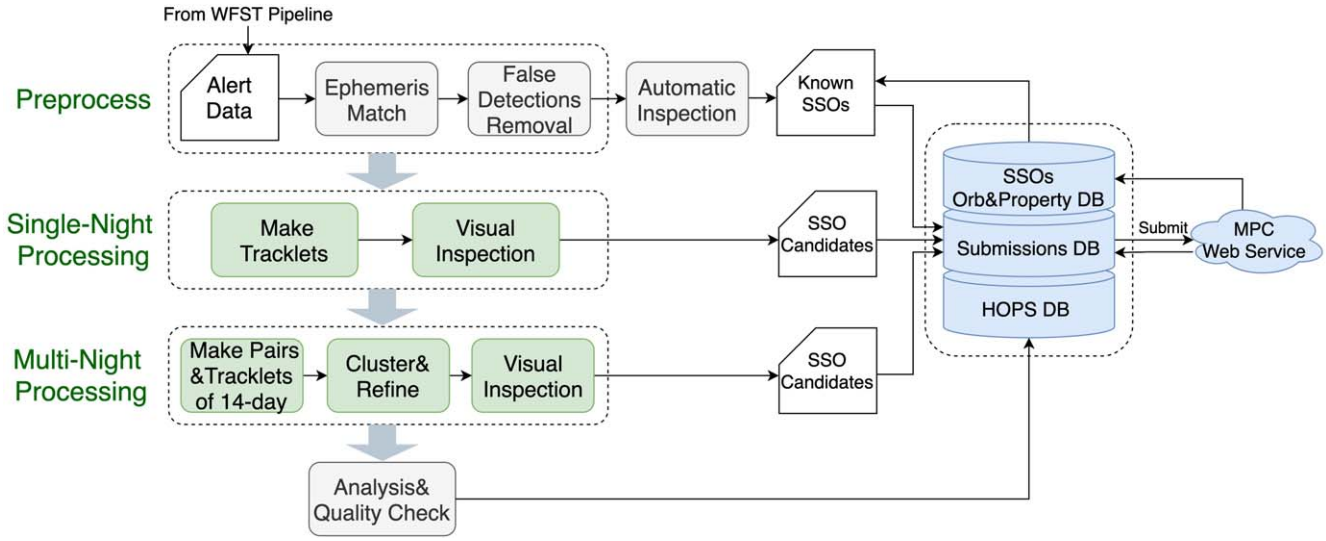

Figure 1. Overview of HOPS architecture. Data processing proceeds in the direction of the arrows shown in the figure.

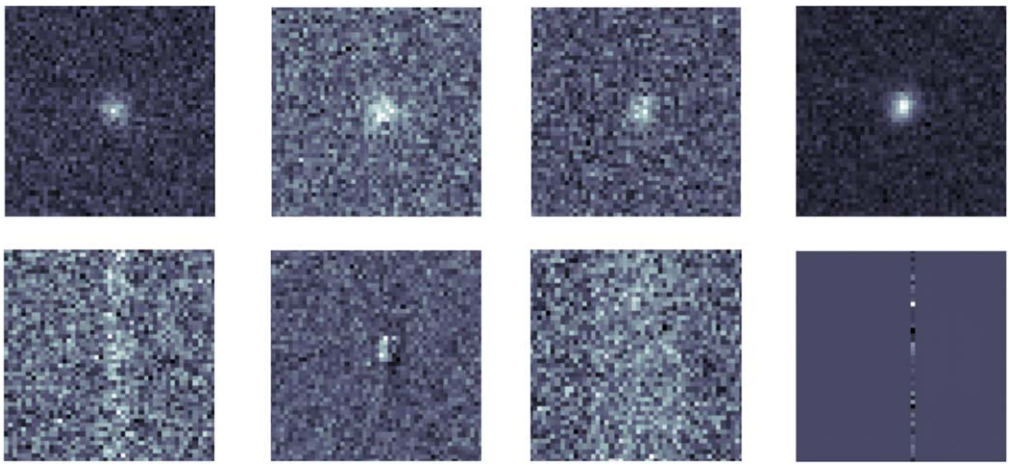

Figure 2. Some example cutouts of true and false sources. The top row shows true sources and the bottom row shows false sources.

2.2. Searching and Analysis

The open-source software `HelioLinC3D`[14], based on the HelioLinC algorithm (M. J. Holman et al. 2018), has been incorporated into HOPS and enables HOPS to operate in two distinct processings: single-night and multinight processing.

2.2.1. Single-night Processing

For data collected over a single night, HOPS invokes `make_tracklets`, which generates pairs and tracklets based on a configuration file specifying speed and arc length criteria. To validate a tracklet, `make_tracklets` applies a least-squares fit, assuming that the object's motion follows a great circle with constant angular velocity see footnote (14). As a result, the tracklets consisting of at least three detections is extracted.

2.2.2. Multinight Processing

For multinight processing, HOPS uses a sliding 14 days window, incorporating data from the past 13 nights plus the current night. The `make_tracklets` function generates all possible pairs and tracklets. `HelioLinC3D` then converts these into three-dimensional "state vectors" using hypothesized heliocentric distances and velocities. These vectors are transformed to a common reference time and clustered. Finally, the `link_refine` function filters out redundant clusters, yielding a deduplicated set of candidate discoveries with high likelihood of being real see footnote (14). `HelioLinC3D` exhibits excellent scalability by identifying clusters with at least two observations per night over at least three nights (referred to as $2+2+2$ mode), as well as in the $2+4$ mode and $3+3$ mode.

2.2.3. Analysis

We evaluate the completeness of HOPS by measuring the fraction of discoverable known SSOs it independently rediscovers without prior knowledge. Software `difi`[15] is used to calculate completeness, defined as the ratio of *found_pure* objects (those found and classified as pure) in the search results of Sections 2.2.1 and 2.2.2, to the *findable* objects identified in the known SSOs matched from Section 2.1.2. In single-night processing, a *findable* object requires a minimum of three

[14] https://github.com/lsst-dm/heliolinc2

[15] https://github.com/moeyensj/difi

observations. In multinight processing, clusters that meet or exceed the 2 + 2 + 2 mode are taken into account. Additionally, *pure_unknown* clusters (all observations are marked as "unknown") are extracted and considered as SSO candidates.

2.3. Inspection and Submission

For known SSOs, HOPS automatically inspects them and removes false detections. SSOs are not expected to change brightness significantly between detections on the same night. Using simplified magnitude conversion formulas from L. Denneau et al. (2013) and R. L. Jones et al. (2018) to convert to Johnson's V band (originally for a mean S+C spectral type), we roughly assess all asteroid types in our matched SSOs. The transformed V band from the observed magnitude is denoted as V_{tr} and calculated as follows: (1) $V_{\rm tr} = g - 0.28$, (2) $V_{\rm tr} = r + 0.23$, (3) $V_{\rm tr} = i + 0.39$, (4) $V_{\rm tr} = z + 0.37$ and (5) $V_{\rm tr} = u - 1.8$ (L. Denneau et al. 2013; R. L. Jones et al. 2018). We exclude observations if the brightness differs by more than 1.0 mag from $V_{\rm ast}$ (see 2.1.2) or if the $V_{\rm tr}$ range exceeds 1.0 mag. In the latter case, the observation that deviates most from the median $V_{\rm tr}$ is removed.

For SSO candidates, we visually inspect gifs of each SSO candidate using an interactive website that displays them alongside relevant information.

Finally, for both known SSOs and SSO candidates, they are cross matched with previously submitted entries in our database (see Section 2.4). If a match is found within 10 s in time and 10″ in angular distance, the detection is discarded to avoid duplicate submissions. Those known SSOs and SSO candidates retained with at least two detections are converted to the 80 column format and submitted to the MPC.[16,17,18] In total, there are three kinds of submissions: (1) single-night known asteroids, (2) single-night SSO candidates, and (3) multinight SSO candidates.

2.4. Database

We employ `MongoDB`, a document-oriented, flexible, and high-performance NoSQL database. Via the `Pymongo` module, the HOPS database manages critical files and results, including sources, their measurements, and linkages. Furthermore, a submission database records acknowledgments and verifications for observations submitted to the MPC. An orbit and identification database is also set up to handle the orbital information of SSOs derived from the daily updated *MPCORB.DAT* file. These databases facilitate the convenient management and association of verifications and orbital data from the MPC with sources and their astrometric data within the HOPS system, thereby supporting future research.

3. Results

From 2024 March 1 to 2024 May 31, HOPS was applied to the observational data collected during the WFST pilot survey in real time. In this section, we present the application of HOPS, its performance metrics, and statistical results for SSOs.

3.1. Applications and Performances

Following the completion of data processing by the WFST pipeline each morning, the alert products generated from the difference images collected throughout the night are automatically transferred to HOPS. As described in Section 2, HOPS begins with preprocessing steps, including known asteroids matching using `astcheck`, and false detection removal using machine learning.

HOPS then performs the single-night and multinight processing and analyzes the results using `difi` (see Section 2.2). In single-night processing, most dates achieve a completeness rate exceeding 95%. The run time of HOPS for all nights is less than 8000 s, and each execution of `HelioLinC3D` reliably completes in less than 20 s, as illustrated in Figure 3. In multinight processing, the total processing time for each night in multinight processing is less than 2000 s (see Figure 4). In multinight processing, HOPS uses preprocessed data from the false detection removal step (Section 2.1.3), with most of the time spent on running `HelioLinC3D`, while a lesser fraction is devoted to data reading and writing operations. Most dates achieve a completeness rate that exceeds 90%.

Subsequently, the processing results, including both known SSOs and SSO candidates, undergo inspections. Inspection of known SSOs is a rapid process that typically takes only a few seconds. SSO candidates can reach up to several hundred per day, with most confirmed as genuine after inspections. Inspecting each candidate's image by eye typically takes just a few seconds.

In practical applications, although the false positive rate is maintained within an acceptable range during the false detection removal phase, the application of this model to real-world data still yields a considerable number of false positives. This phenomenon is ascribed to the exclusion of numerous potential conditions from the training samples. To mitigate this issue, an enhancement of the dataset used for machine learning is planned in future iterations.

3.2. Alert Data and Preprocessed Results

During the period, HOPS processed a total of 60,266,765 alert entries. After removing false detections, the number of preprocessed alert entries decreased to 1,993,506, representing approximately 3.31% of the initial dataset. The `astcheck` matching process successfully identified a total of 888,286 alerts corresponding to 38,879 SSOs as confirmed SSOs.

3.3. Known Asteroids

The wide field of view of the WFST, combined with its strong survey capabilities, allows us to gather extensive observational data on known SSOs. During the period from 2024 March 1 to 2024 May 31, there were 658,489 observations of 38,520 known asteroids verified by the MPC in our submissions. Of the 38,520 identified known asteroids, the orbital distributions of 38,474 asteroids with various orbit types that are described in the MPC files are illustrated in Figure 5. The results of known SSOs recognized by the MPC after processing our submissions consist of: (1) known SSOs that are matched by *astcheck* and submitted directly, and (2) a subset of SSO candidates that were initially not matched within our pipeline but were subsequently identified as known asteroids by the MPC.

[16] https://www.minorplanetcenter.net/iau/info/OpticalObs.html
[17] https://www.minorplanetcenter.net/iau/info/ObsDetails.html
[18] https://www.minorplanetcenter.net/iau/info/commandlinesubmissions.html

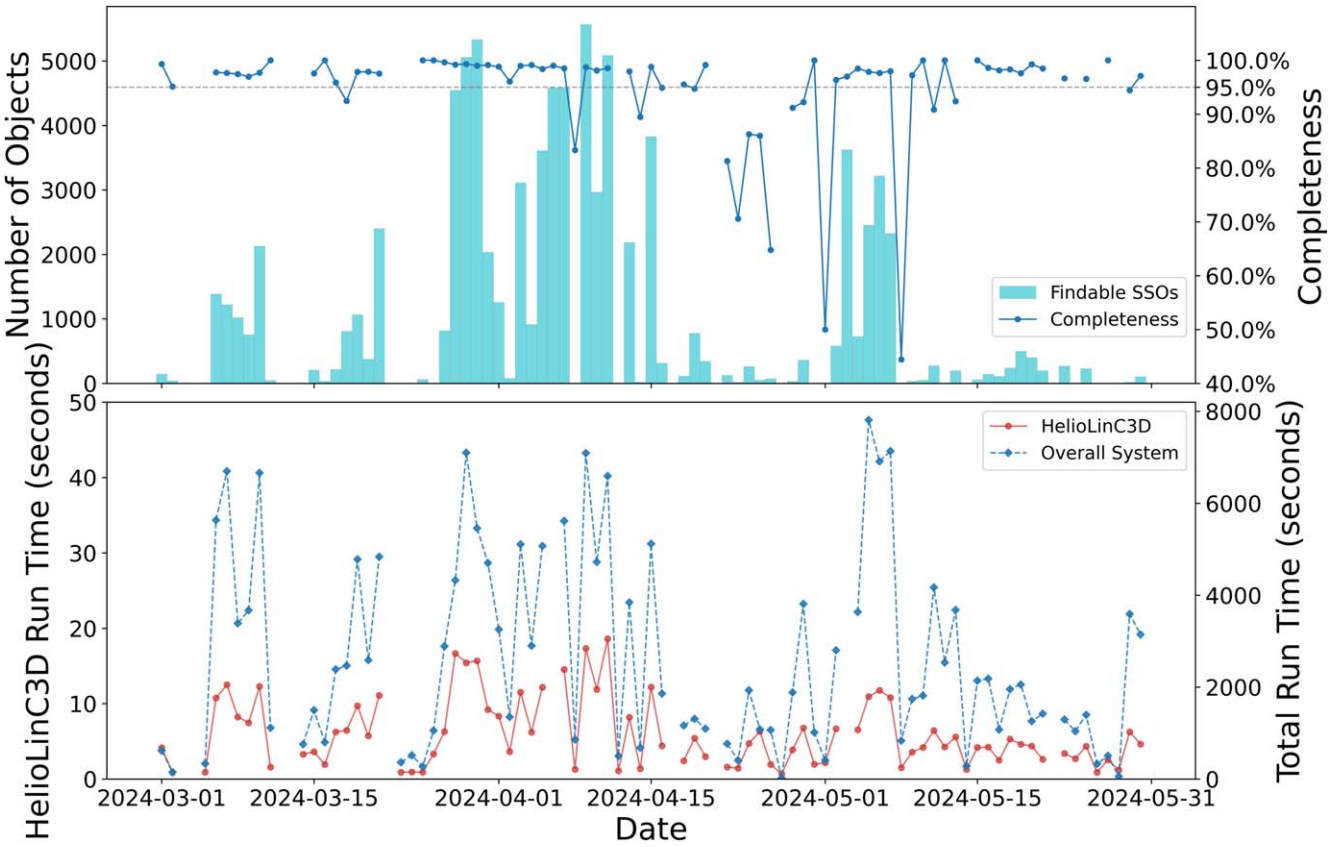

Figure 3. Completeness and run times of HOPS in single-night processing. Top: the number of findable SSOs and completeness of HOPS over dates. The gray line is 95.0% completeness. Bottom: run time of the `HelioLinC3D`'s *make_tracklets* (red dot) and the entire HOPS over dates (blue diamond).

3.4. New Asteroids

In the course of the WFST pilot survey, we submitted a cumulative total of 81 batches concerning SSO candidates to the MPC, covering 5875 linkages and 24,036 observations. Upon verification by the MPC, 241 new asteroids received provisional designations and were initially reported by the WFST (see Figure 6). Furthermore, 2125 observations were recorded in the ITF and are pending further observational data for linkage.

On the one hand, for single-night processing, there are 35 batches based solely on data from single-night observations, comprising 3341 linkages with 11,456 observations. From these submissions, 24 new asteroids were confirmed by the MPC using only single-night observation data. On the other hand, the remaining 46 batches utilized data from multinight observations, accounting for 2534 linkages and 12,580 observations (see Table 1). In particular, 27% of all newly identified asteroids confirmed by the MPC were discovered using the $2 + 2 + 2$ mode. In this case, HelioLinC3D has been proven to be effective and efficient when applied to our wide field survey data.

4. Summary

This work details the architecture, design, and processing flow of the HOPS using the innovative HelioLinC3D algorithm and presents initial results from its application to the WFST pilot survey. HOPS is capable of identifying known asteroids and searching for SSO candidates through both single-night and multinight processing. Using data from a three-month pilot survey, we reported 658,489 observations of 38,520 objects of known asteroids and 24,036 observations of 5875 linkages of SSO candidates. A total of 241 newly discovered asteroids received provisional designations from the MPC, while 2125 observations were placed into the MPC's ITF for further confirmation. Notably, 27% of the newly identified asteroids were identified exclusively in the $2 + 2 + 2$ mode.

The results also underscore the notable performance of HOPS in time efficiency and completeness, effectively managing both single-night and multinight processing. The successful application of HelioLinC3D to WFST, particularly in multinight processing, demonstrates the algorithm's efficiency and productivity in the context of wide field surveys, backed by extensive real-world data. Furthermore, WFST is emerging as a significant contributor to asteroid detection, showing considerable promise in advancing the study of solar system research.

HOPS continuously processes data and undergoes ongoing optimization with openness to advanced tools. Future enhancements aim to improve data quality by addressing poor photometry, reducing false detections, and refining machine learning data sets and models. The accuracy of matching known SSOs will be enhanced using optimized ephemeris tools such as Aleph (J. Peña Zamudio & C. Fuentes 2021). Moreover, we plan to integrate HOPS with orbit determination tools to validate high-quality tracklets, enable searches for special SSOs, and support the monitoring of Potentially Hazardous Asteroids. The new ADES format for MPC submissions, along with the advanced HeliolincRR tool,[19] is considered to be tested and integrated into HOPS. We will also develop reliable

[19] https://github.com/bengebre/heliolincrr

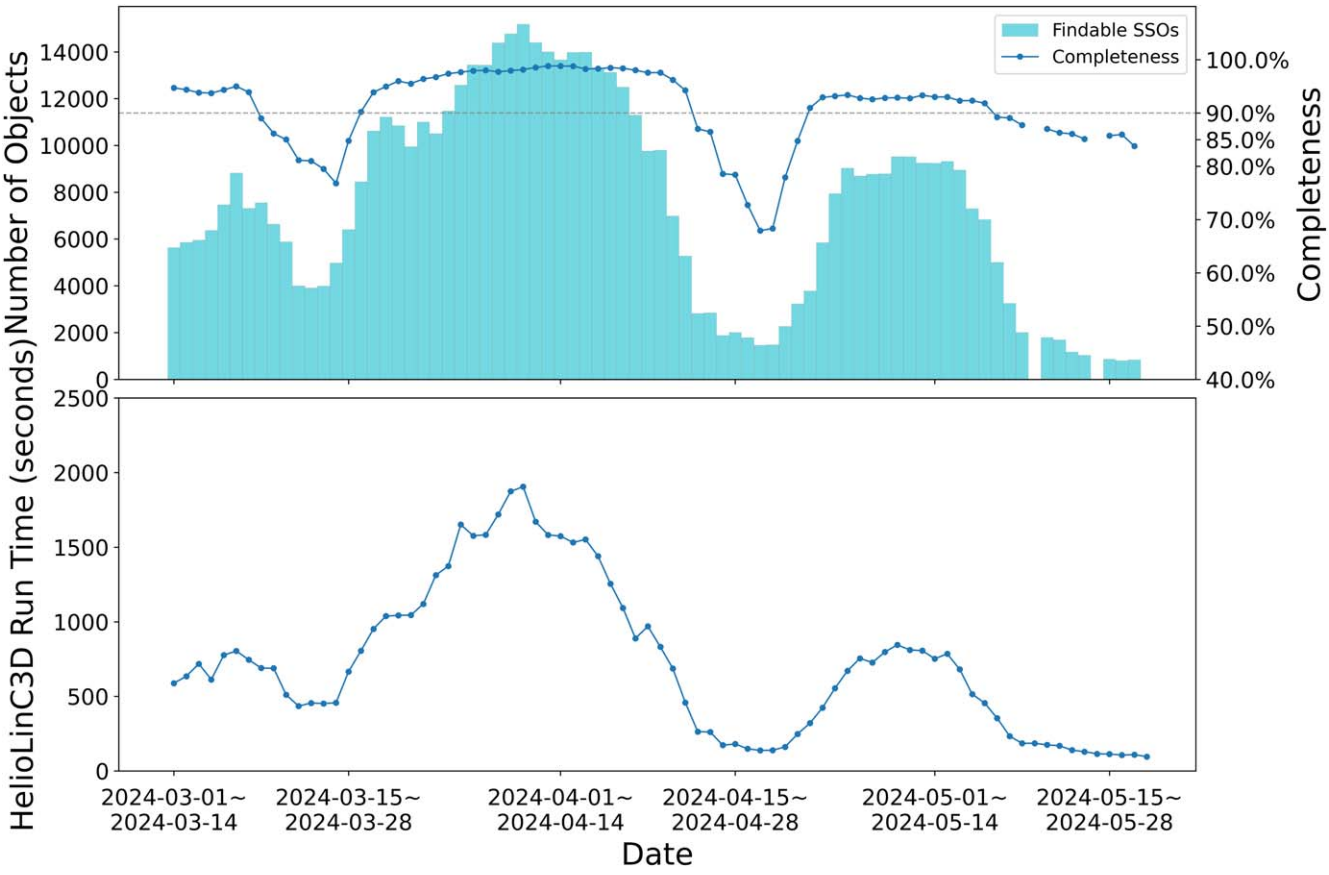

Figure 4. Completeness and run times of HOPS in multinight processing. Top: the number of findable SSOs and the completeness of HOPS over dates. The gray line is 90.0% completeness. Bottom: run times of the `HelioLinC3D` over dates.

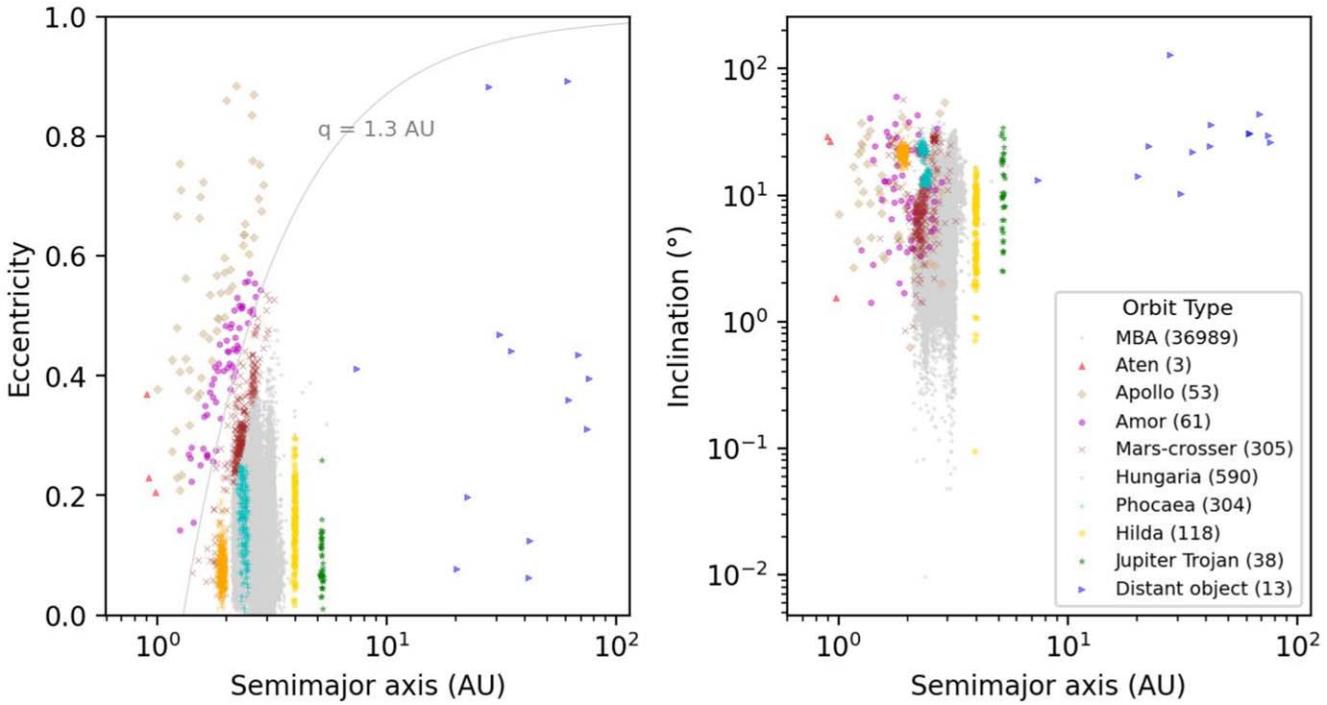

Figure 5. Orbital elements distribution of various types of 38,474 known asteroids observed by WFST, marked with different symbols. Left: the distribution of eccentricity vs. semimajor axis, with a gray line indicating the orbital elements where q (perihelion distance) equals 1.3 au. Right: the distribution of inclination vs. semimajor axis.

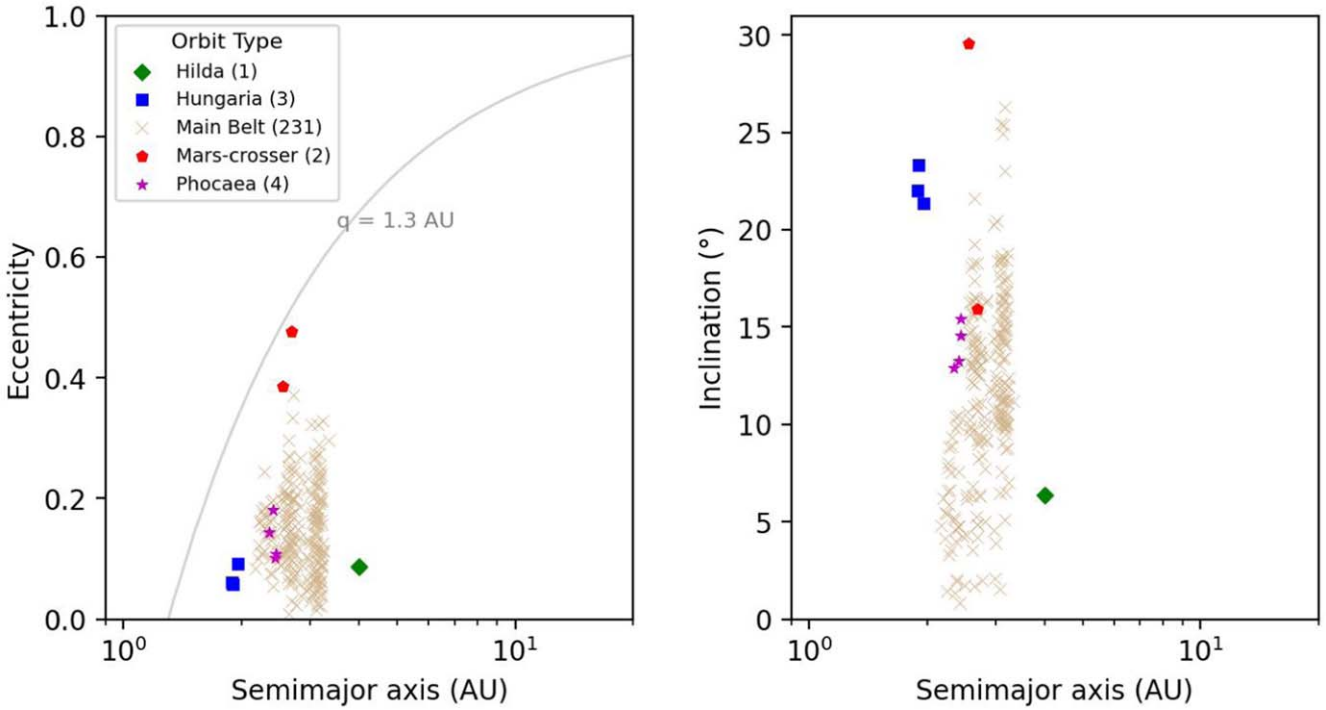

Figure 6. Orbital elements distribution of various types of SSO candidates initial reported by WFST, marked with different symbols. Left: the distribution of eccentricity vs. semimajor axis, with a gray line indicating the orbital elements where q (perihelion distance) equals 1.3 au. Right: the distribution of inclination vs. semimajor axis.

Table 1
WFST Results on Submitted SSO Candidates in the Pilot Survey

Observation Type	Number of Batches	Number of Observations	Number of Linkages	Number of New Asteroids
Single-night data	35	11456	3341	24
Multinight data	46	12580	2534	217
Total	81	24036	5875	241

and user-friendly interfaces to streamline subsequent SSO research workflows.

While HOPS takes the initial step by acquiring astrometric data of SSOs, deriving scientific insights requires a deeper analysis. This involves understanding the scientific context and physical properties of the entire asteroid population, serving two complementary goals: identifying global trends, such as light-curve periods, amplitudes, size, and color, from accumulated data and searching for rare events. To achieve these goals, executable steps involve comparing an object's observed behaviors with its expected behavior and contrasting each object against the ensemble to identify those with unusual properties (D. E. Trilling et al. 2023). Significant efforts are needed to fully exploit the substantial data from WFST. Other technologies being considered include machine learning to detect NEO streaks (Q. Ye et al. 2019), monitoring activity using machine learning (D. A. Duev et al. 2021; C. Chandler et al. 2024), and employing wedge photometry (C. O. Chandler et al. 2021) to detect tails from cutouts. Furthermore, we plan to integrate advanced tools such as Kernel-Based Moving Object Detection (P. J. Whidden et al. 2019; H. Smotherman et al. 2021) and sbpy (M. Mommert et al. 2019) for further research. We believe that these strategies can significantly enhance the potential of WFST in a wider range of solar system research domains.

Acknowledgments

The authors thank the anonymous referee for their valuable comments and constructive feedback, which have greatly improved the quality of this manuscript. We are deeply grateful to Peter Vereš and the Minor Planet Center (MPC) for their invaluable feedback and insightful suggestions on improving our system. The Wide Field Survey Telescope (WFST) is a joint facility of the University of Science and Technology of China, Purple Mountain Observatory. This work is supported by National Key Research and Development Program of China (2023YFA1608100) and the Strategic Priority Research Program of Chinese Academy of Sciences, grant No. XDB 41000000. The authors gratefully acknowledge the support of the National Natural Science Foundation of China (NSFC, grant No. 12173037, 12233008), the CAS Project for Young Scientists in Basic Research (No. YSBR-092), the Fundamental Research Funds for the Central Universities (WK3440000006), Cyrus Chun Ying Tang Foundations and the 111 Project for "Observational and Theoretical Research on Dark Matter and Dark Energy" (B23042).

Facility: WFST: 2.5 m

Software: `astropy` (Astropy Collaboration et al. 2013, 2018, 2022), `Jupyter` (F. Perez & B. E. Granger 2007; T. Kluyver et al. 2016), `matplotlib` (J. D. Hunter 2007), `numpy` (C. R. Harris et al. 2020), `pandas` (W. McKinney 2010; The pandas development team 2024), `python`

(G. Van Rossum & F. L. Drake 2009), `scipy` (P. Virtanen et al. 2020; R. Gommers et al. 2024), `HelioLinC3D` (M. J. Holman et al. 2018), `difi` (J. Moeyens 2021), `astcheck` (B. Gray 2022), `braai` (D. A. Duev et al. 2019) and `mongodb` (MongoDB Inc. 2024)

ORCID iDs

Shao-Han Wang https://orcid.org/0009-0007-8133-5249
Bing-Xue Fu https://orcid.org/0000-0003-4122-6949
Jun-Qiang Lu https://orcid.org/0009-0008-4604-9674
LuLu Fan https://orcid.org/0000-0003-4200-4432
Min-Xuan Cai https://orcid.org/0000-0003-4721-6477
Xu Kong https://orcid.org/0000-0002-7660-2273
Ya-Ting Liu https://orcid.org/0009-0008-4858-1410
Qing-feng Zhu https://orcid.org/0000-0003-0694-8946
Zhen Wan https://orcid.org/0000-0002-3105-3821
Ji-an Jiang https://orcid.org/0000-0002-9092-0593
Wentao Luo https://orcid.org/0000-0003-1297-6142
Yongquan Xue https://orcid.org/0000-0002-1935-8104
Wen Zhao https://orcid.org/0000-0002-1330-2329

References

Astropy Collaboration, Price-Whelan, A. M., Lim, P. L., et al. 2022, ApJ, 935, 167
Astropy Collaboration, Price-Whelan, A. M., Sipőcz, B. M., et al. 2018, AJ, 156, 123
Astropy Collaboration, Robitaille, T. P., Tollerud, E. J., et al. 2013, A&A, 558, A33
Brown, P., Assink, J., Astiz, L., et al. 2013, Natur, 503, 238
Cai, M., Xu, Z., Fan, L., et al. 2025, arXiv:2501.15018
Chandler, C., Oldroyd, W., Trujillo, C., et al. 2024, AAS/DPS Meeting Abstracts, 56, 112.04
Chandler, C. O., Trujillo, C. A., & Hsieh, H. H. 2021, ApJL, 922, L8
Christensen, E. J., Carson Fuls, D., Gibbs, A., et al. 2016, AAS/DPS Meeting Abstracts, 48, 405.01
Deng, L., Yang, F., Chen, X., et al. 2021, Natur, 596, 353
Denneau, L., Jedicke, R., Grav, T., et al. 2013, PASP, 125, 357
Duev, D. A., Bolin, B. T., Graham, M. J., et al. 2021, AJ, 161, 218
Duev, D. A., Mahabal, A., Masci, F. J., et al. 2019, MNRAS, 489, 3582
Gomes, R., Levison, H. F., Tsiganis, K., & Morbidelli, A. 2005, Natur, 435, 466
Gommers, R., Virtanen, P., Haberland, M., et al. 2024, scipy/scipy: SciPy, v1.13.1, Zenodo, doi:10.5281/zenodo.11255513
Gray, B. 2022, astcheck asteroid checking software, https://www.projectpluto.com/astcheck.htm
Harris, C. R., Millman, K. J., van der Walt, S. J., et al. 2020, Natur, 585, 357
Holman, M. J., Payne, M. J., Blankley, P., Janssen, R., & Kuindersma, S. 2018, AJ, 156, 135
Hu, M., Hu, L., Jiang, J.-a., et al. 2023, Univ, 9, 7
Hunter, J. D. 2007, CSE, 9, 90
Ivezić, Ž., Kahn, S. M., Tyson, J. A., et al. 2019, ApJ, 873, 111
Jones, R. L., Slater, C. T., Moeyens, J., et al. 2018, Icar, 303, 181
Jurić, M., Kantor, J., Lim, K. T., et al. 2017, in ASP Conf. Ser. 512, Astronomical Data Analysis Software and Systems XXV, ed. N. P. F. Lorente, K. Shortridge, & R. Wayth (San Francisco, CA: ASP), 279
Kluyver, T., Ragan-Kelley, B., Pérez, F., et al. 2016, in Positioning and Power in Academic Publishing: Players, Agents and Agendas, ed. F. Loizides & B. Schmidt (Amsterdam: IOS Press), 87
Kurlander, J. A., Holman, M. J., Bernardinelli, P. H., et al. 2025, AJ, 169, 73
Lei, L., Zhu, Q.-F., Kong, X., et al. 2023, RAA, 23, 035013
Lin, J., Wang, T., Cai, M., et al. 2024, arXiv:2412.12601
Lin, Z., Jiang, N., & Kong, X. 2022, MNRAS, 513, 2422
Liu, Z.-Y., Lin, Z.-Y., Yu, J.-M., et al. 2023, ApJ, 947, 59
LSST Science Collaboration, Abell, P. A., Allison, J., et al. 2009, arXiv:0912.0201
Lu, J.-Q., Fan, L.-L., Cai, M.-X., et al. 2025, PASP, 137, 024401
McKinney, W. 2010, in Proc. the 9th Python in Science Conf., ed. S. van der Walt & J. Millman (Austin, TX: SciPy), 56
Mahlke, M., Solano, E., Bouy, H., et al. 2019, A&C, 28, 100289
Masci, F. J., Laher, R. R., Rusholme, B., et al. 2018, PASP, 131, 018003
Michel, P., DeMeo, F. E., & Bottke, W. F. 2015, Asteroids IV (Tucson, AZ: Univ. Arizona Press)
Moeyens, J. 2021, difi https://pypi.org/project/difi/
Mommert, M., Kelley, M., de Val-Borro, M., et al. 2019, JOSS, 4, 1426
MongoDB Inc. 2024, MongoDB, https://www.MongoDB.com
Morbidelli, A., Levison, H. F., Tsiganis, K., & Gomes, R. 2005, Natur, 435, 462
Peña Zamudio, J., & Fuentes, C. 2021, AAS/DPS Meeting Abstracts, 53, 306.03
Perez, F., & Granger, B. E. 2007, CSE, 9, 21
Raymond, S. N., & Izidoro, A. 2017, SciA, 3, e1701138
Schwamb, M. E., Jones, R. L., Chesley, S. R., et al. 2018, arXiv:1802.01783
Smotherman, H., Connolly, A. J., Kalmbach, J. B., et al. 2021, AJ, 162, 245
Su, Z.-B., Cai, Z.-Y., Wang, J.-X., et al. 2024, ApJ, 976, 155
The pandas development team 2024, pandas-dev/pandas: Pandas, v2.2.2, Zenodo, Zenodo: 10.5281/zenodo.10957263
Trilling, D. E., Gowanlock, M., Kramer, D., et al. 2023, AJ, 165, 111
Tsiganis, K., Gomes, R., Morbidelli, A., & Levison, H. F. 2005, Natur, 435, 459
Van Rossum, G., & Drake, F. L. 2009, Python 3 Reference Manual (Scotts Valley, CA: CreateSpace)
Virtanen, P., Gommers, R., Oliphant, T. E., et al. 2020, NatMe, 17, 261
Walsh, K. J., Morbidelli, A., Raymond, S. N., O'Brien, D. P., & Mandell, A. M. 2011, Natur, 475, 206
Wang, T., Liu, G., Cai, Z., et al. 2023, SCPMA, 66, 109512
Whidden, P. J., Kalmbach, J. B., Connolly, A. J., et al. 2019, AJ, 157, 119
Ye, Q. 2024, arXiv:2409.09540
Ye, Q., Masci, F. J., Lin, H. W., et al. 2019, PASP, 131, 078002